

COMPARISON OF SNS SUPERCONDUCTING CAVITY CALIBRATION METHODS *

Y. Zhang, I. Campisi, P. Chu, J. Galambos,
S. D. Henderson, D. Jeon, K. Kasemir, A. Shishlo
Spallation Neutron Source, ORNL, Oak Ridge, TN 37831, USA

Abstract

Three different methods have been used to calibrate the SNS superconducting cavity RF field amplitude. Two are beam based and the other is strictly RF based. One beam based method uses time-of-flight signature matching (phase scan method), and the other uses the beam-cavity interaction itself (drifting beam method). Both of these methods can be used to precisely calibrate the pickup probe of a SC cavity and determine the synchronous phase. The initial comparisons of the beam based techniques at SNS did not achieve the desired precision of 1% due to the influence of calibration errors, noise and coherent interfaces in the system. To date the beam-based SC cavity pickup probe calibrations agree within approximately 4%, comparable to the conventional RF calibrations.

RF CALIBRATION

A schematic drawing of the SNS superconducting cavity RF system is shown in figure 1. Each RF cavity unit includes a 550 kW klystron, a Low Level RF (LLRF) cavity control system and an 805MHz niobium cavity which has four RF ports: Power Coupler (PC), Field Probe (FP), High Order Mode (HOM) couplers HOM A and HOM B. The LLRF system consists of a High Power Protection Module (HPPM) and a Field Control Module (FCM) [1].

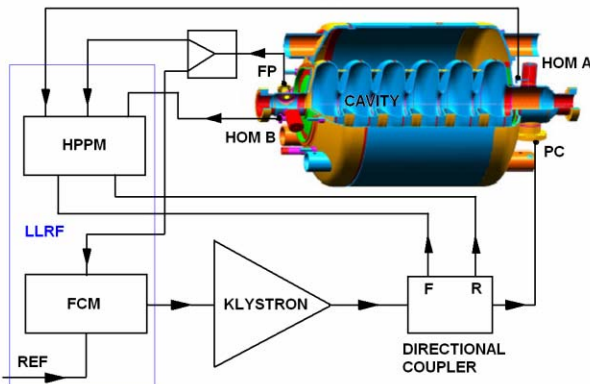


Figure 1: Schematic drawing of the cavity RF system.

Table 1: Design parameters of SNS cavity

	Medium beta	High beta
Loaded Q	7.3×10^5	7.0×10^5
Active length	0.682 m	0.906 m
R/Q	278.6 Ω	483.6 Ω
$T(\beta_{opt})$	0.681	0.701

* SNS is managed by UT-Battelle, LLC, under contract DE-AC05-00OR22725 for the U.S. Department of Energy.

In baseline design, acceleration gradient for medium beta cavity ($\beta=0.61$) is 10.1 MV/m and for high beta cavity ($\beta=0.81$) is 15.9 MV/m. Some other design parameters are listed in table 1.

RF calibration is performed with the LLRF system at different powers and for different pulse lengths, by measuring power in each RF port of the cavity, as well as comparing with the cavity stored energy measurements obtained from integration of transmitted powers in the field probes. Equations used in the RF calibrations are:

$$E_a = \sqrt{\frac{R/Q}{L^2} \cdot 4 \cdot Q_L \cdot P_F} \quad \text{forward long pulse}$$

$$E_a = \sqrt{\frac{R/Q}{L^2} \cdot 4 \cdot Q_L \cdot P_R} \quad \text{reflected long pulse}$$

$$E_a = \sqrt{\frac{R/Q}{L^2} \cdot 4 \cdot Q_{ext} \cdot P_T} \quad \text{transmitted pulse}$$

$$E_a = \sqrt{\frac{R/Q}{L^2} \cdot \omega_{rf} \cdot U_{cav}} \quad \text{emitted short pulse}$$

where, L is the cavity active length listed in table 1, R/Q is also listed in the table, Q_L is the cavity loaded quality factor, Q_{ext} is the external quality factor of the field probe, P_F , P_R and P_T , are the forward power, the reflected power and the transmitted power respectively, and U_{cav} is the cavity stored energy.

The measured results with transmitted powers from cavity field probes, with forward RF powers and reflected powers of the cavity are usually in a close agreement with cavity stored energy measurement (less than 10%) as RF powers dissipated in the SC cavity can be ignored. However, the cavity gradient measured with the two HOM couplers often differs more, because the design rejects the fundamental mode. The RF calibration referenced here is measured with the cavity field probe, and the average acceleration gradient of all available SNS cavities reached a maximum of 17.6 MV/m [2].

PHASE SCAN

Phase scan signature matching [3] is based on time-of-flight measurement. Since the particle energy gain and resulting cavity-exit velocity depends on the cavity phase, the cavity phase is scanned and the phase difference between two downstream beam phase monitors (BPMs) is measured accordingly. By fitting the measured result of BPM phase difference curve with a model one may get

beam energy, cavity phase, and field amplitude precisely [4]. But the method may not apply for highly relativistic particles when beam velocity change is too small. Furthermore, it also needs to account for beam loading in unpowered SC cavities for high current beams [5, 6].

The SNS cavity has six cells, and nonlinear effects exist in particle accelerations so that the measured curve is not a pure sinusoidal one. But fitting of the BPM measurement may still use a simple RF cavity model:

$$W_{out} = W_{in} + E_a \cdot \cos(\phi_{rf} + \phi_0)$$

More sophisticated RF cavity models are also possible. Step integration methods, slicing the cavity field profile into thousands of tiny steps, and Runge-Kutta or other numerical methods could be used to solve the differential equations of charged particle motions in an RF field. However, those methods are time-consuming. Practically, the required accuracy is achieved quickly with a thin lens approximation [7] – The particle is assumed to travel at constant velocity to the cavity center, where it receives a longitudinal kick and is then transported out of the cavity at a new velocity:

$$\Delta W = qE_0 \cdot T \cdot L \cdot \cos \phi_s$$

$$\Delta \phi = \frac{qE_0 \cdot L}{mc^2 \cdot \beta^2 \cdot \gamma^3} k \cdot T' \cdot \sin \phi_s$$

$$\phi_s = \phi_0 + l_1 \cdot \frac{d\phi_0}{ds} - \frac{\pi \cdot qE_0 \cdot L}{mc^2 \cdot \beta_h^2 \cdot \gamma_h^3} \cdot [T' \cdot \sin \phi_c + S' \cdot \cos \phi_c]$$

where, k is the wave number, l_1 is the distance from the cavity entrance to the center, ϕ_0 is the RF phase at the cavity entrance, β and γ are the relativistic factors at the center while β_h and γ_h are those at the first half cavity, T , T' and S' are the transit-time factors and their derivatives, and $\Delta \phi$ is the phase kick due to beam acceleration.

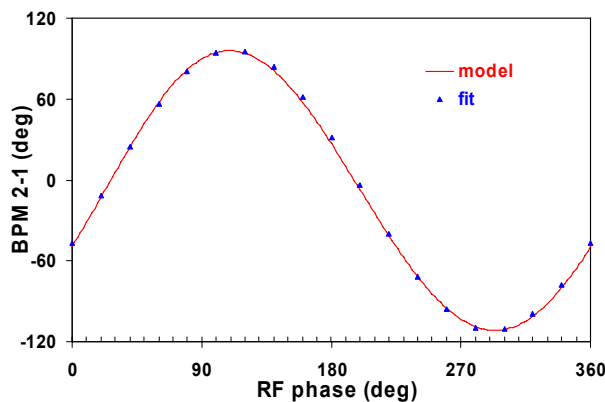


Figure 2: Phase scan of a cavity for 186 MeV beams.

Figure 2 shows a simulated BPM curve in phase scan and the fitting with a sinusoidal function. In principle, cavity field probe calibration with phase scan signature matching may reach an accuracy of up to $\pm 1\%$. However, it is compromised by calibration errors of BPMs and by noise in the LLRF measurement. At SNS, a phase scan

measurement with different BPM pairs and for different beam currents and pulse lengths shows that the actual accuracy reached is approximately 2.4%.

DRIFTING BEAM

The drifting beam technique is based on very strong beam-cavity interactions in the SC cavity for high current beams. It was proposed several years ago [8] and recently realized at SNS [9, 10]. It uses measured beam currents and pulse shapes with a beam current monitor (BCM), and beam induced signals in the SC cavity with the cavity control circuit. Using the measured beam current in a beam-cavity model that simulates the beam-loading in the cavity, by comparing model simulation results with the actual measurement of the cavity, cavity phase and the field amplitude are determined precisely. In principle, the accuracy is also up to $\pm 1\%$.

In the equivalent RLC circuit of an RF cavity, beam loading in an unpowered cavity equals to:

$$V = V_L + \frac{1}{2} V_{b0}$$

$$V_L = V_{b0} \cdot \left\{ \exp\left[-T_b \left(\frac{1}{T_F} + j \cdot d\omega\right)\right] + \dots \right\}$$

$$V_{b0} = I(\omega) \cdot R_{sh} \cdot \frac{T_b}{T_F}$$

where, T_b is the beam bunch period, T_F is the filling time of the cavity, R_{sh} is the shunt impedance ($=Q_L \cdot R/Q$), I is the image current of the beam bunch in the frequency domain, which may be obtained from Fourier transform of the time domain beam current, ω is the angular frequency, and $d\omega$ is the cavity detuning.

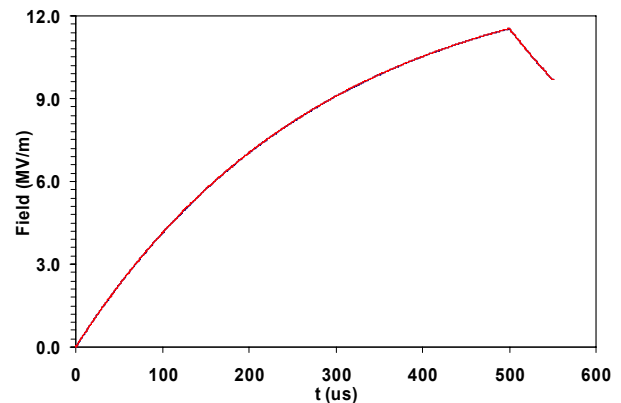


Figure 3: Field induced by a 750MeV and 52mA beam with pulse length 500 μ s, in a high beta SNS cavity.

Figure 3 shows beam induced field in an SC cavity for 750MeV and 52mA beams with pulse length of 500 μ s, from simulations with the beam-cavity model. Beam induced signals in the cavity include HOMs and other passband modes of the TM010 mode in addition to the fundamental acceleration mode, and can be ignored in the drifting beam calibration when pulse length $\geq 50 \mu$ s.

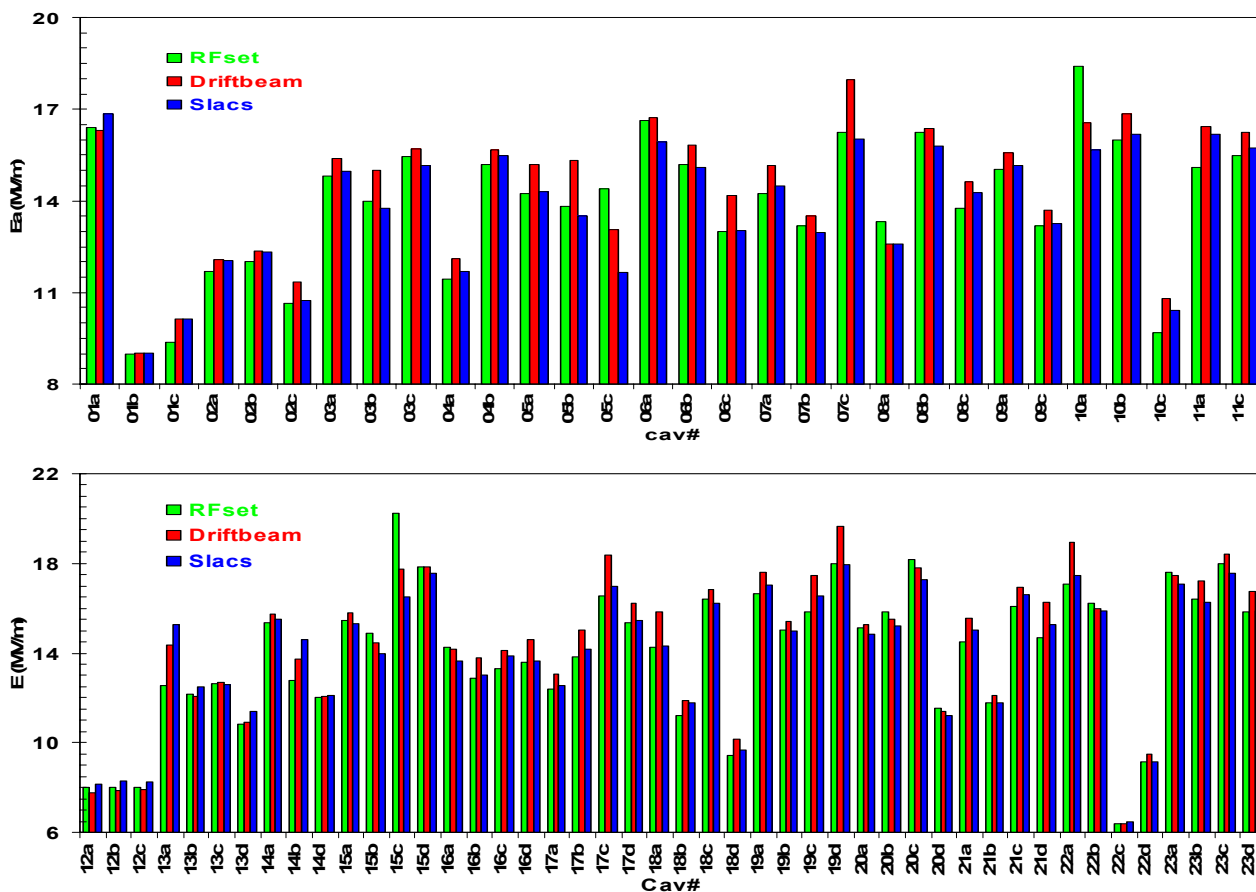


Figure 4: Acceleration gradient of all the available SNS cavities from RF calibrations (RF set) and from beam-based calibrations: drifting beam (driftbeam) and phase scan (Slacs). Averaged 14MV/m. (80% of the max. 17.6MV/m).

RESULTS

Initial calibration results of all the available SNS cavities with conventional RF calibrations and with beam-based measurements are shown in figure 4. Acceleration gradients averaged 14MV/m, which is approximately 80% of the maximum tested gradient. The results show that RF calibration reached the limit of $\pm 5\%$ - the difference to the more accurate beam based calibrations, while drifting beam and phase scan calibration is within $\pm 4\%$ (rms).

As we discussed previously, phase scan is influenced by BPM calibrations, drifting beam is mainly affected by BCM calibrations: using a different BCM, the result of drifting beam measurement could be 10% different. After precise calibrations for a few BCMs with an estimated accuracy of approximately $\pm 3\%$, we have better drifting beam measurements. However, the average acceleration gradient in drifting beam measurement is 14.4MV/m, 3% higher than that of phase scan or RF calibration.

Besides BPMs and BCMs, many factors significantly influence beam based calibrations, e.g., bunch size, beam phase/energy jitter, cavity detuning, beam loadings in unpowered SC cavities, noise and coherent interface in the LLRF system cross talk. Many efforts remain to improve the calibration accuracy to $\pm 1\%$, but observed beam loss at the present resolution is acceptable for present beam power levels.

CONCLUSION

In SNS beam commissioning, the initial results of beam based calibrations of SC cavity RF amplitudes are promising. Phase scan and drifting beam techniques are successfully tested with accuracy comparable to the RF calibration. Work is still needed to improve the precision.

REFERENCES

- [1] H. Ma, et al., PRST-AB, **9**, 032001 (2006).
- [2] I. E. Campisi, Proceedings of 2005 Particle Accelerator Conference, Knoxville, USA, 2005, p34.
- [3] T. L. Owens, et al., Particle Accelerators, Vol. **48** (1994) 169.
- [4] J. Galambos, et al., Proceedings of 2005 Particle Accelerator Conference, Knoxville, USA, 2005, p1491.
- [5] S. D. Henderson, et al., Proceedings of 2005 Particle Accelerator Conference, Knoxville, USA, 2005, p3423.
- [6] D. Jeon, et al., these proceedings.
- [7] B. Schnizer, Particle Accelerators, Vol. **2** (1971) 141.
- [8] L. Young, Proceedings of 2001 Particle Accelerator Conference, Chicago, USA, 2001, p572
- [9] Y. Zhang, et al., to be published.
- [10] P. Chu, Y. Zhang, these proceedings.